

CIV102 Bridge Report

Oscar Sun, Syeda Mahdia, Di Hu
November 26th, 2023

1 Introduction

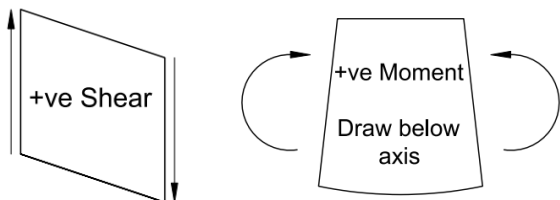
A small-scale box girder bridge with a span of 1270 mm was designed out of matboard. Based on design iterations done prior to the final version, the bridge was designed primarily with the goal of maximizing factors of safety against matboard compression failure and top flange buckling failure. This was achieved by increasing the web height and tab widths glued to the top flange. Construction details such as matboard cutting, number of possible diaphragms from left over areas, and number and location of distinct splices was also factored into bridge constructions. The final bridge design has a factor of safety of 2.60, which reflects a theoretical failure load of 1041 N.

Key Design Decisions

- Make the bridge as tall as possible-if permissible-by matboard cutting
- Use box girders for cross-section design. Main variations in box girder cross sections include width of glue tabs, web heights, whether to adapt C-shaped or U-shaped webs.
- Keep bridge height consistent throughout for easier construction. Since main failure modes are dominated by sections of the bridge with lower heights, increasing the factor of safety at higher bridge sections does not necessarily make the design superior to bridges with consistent heights.
- The spacing between webs will be equal to train width (approx. 75mm) so that the train weight is directly supported by the webs underneath.
- Incorporate more diaphragms close to bridge support because diaphragms are better at resisting shear stress. Incorporate diaphragms for stiffening the box girder cross section.
- Increase the glue tab width underneath the top flange such that there are no gaps in between the glue tabs. This effectively doubles the thickness t in the top flange buckling equation, resulting in a higher FOS against flange buckling.

Sign Convention

The sign convention provided below applies to all SFDs and BMDs in this design report. SFD has its positive axis upward, whereas BMD has its positive axis downward.

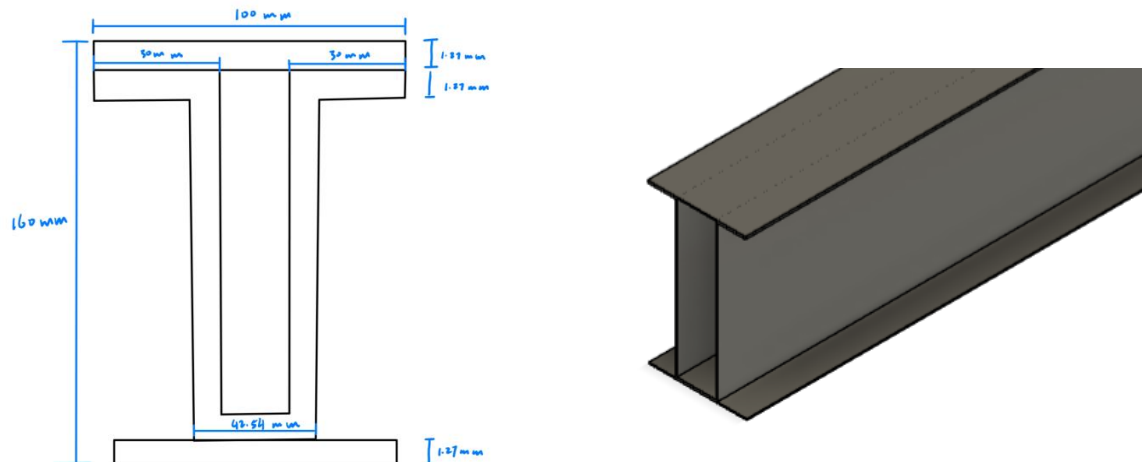


2 Design Iterations

Next to each design, there will be a 3D visualization of it created using Fusion 360.

Design 1: I-shaped cross-section

Visualization:



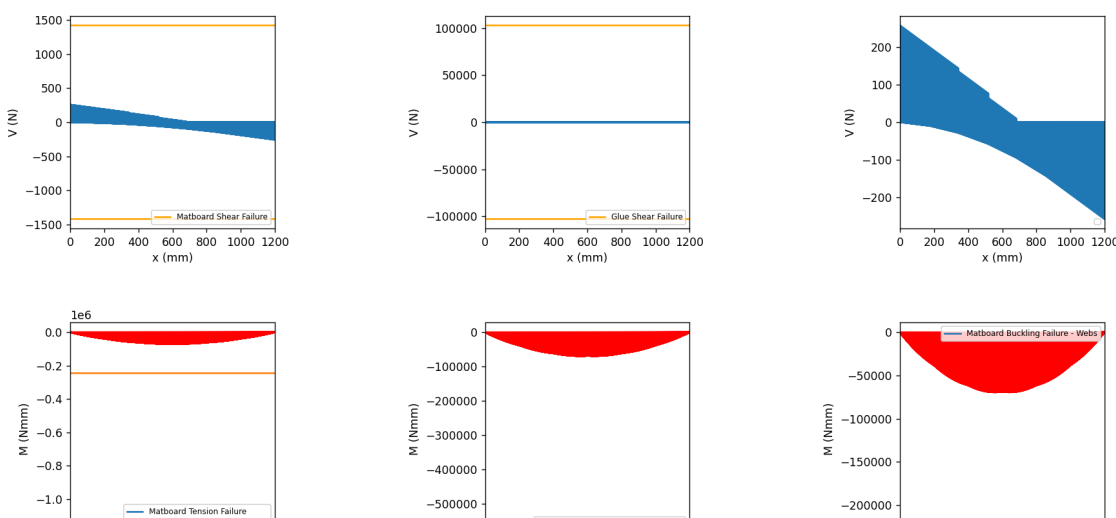
Key parameter(s) altered:

An I-shaped cross-section is used in design 1 instead of the box girder provided in design 0.

Justification:

- An I-shaped cross-section was designed to maximize the second moment of area, I , a variable present in calculations for all modes of failure. I-shaped cross-sections have their main area distributions further from their centroidal axes, increasing I ; a desirable characteristic.
- Given that the width of the matboard is 1.27 mm, it is impractical to have a web with only 1.27 mm in contact with the top and bottom flanges. This reduces the area over which the forces are being felt, as well as the area of the contact cement. Therefore, the web is folded, and has some resemblance to a thin box girder shape. This not only increases the area of contact between the webs, glue and top flange, but also helps decrease the overall stress, as the larger the area over which a force is distributed helps reduce it.

SFDs and BMDs:



Results:

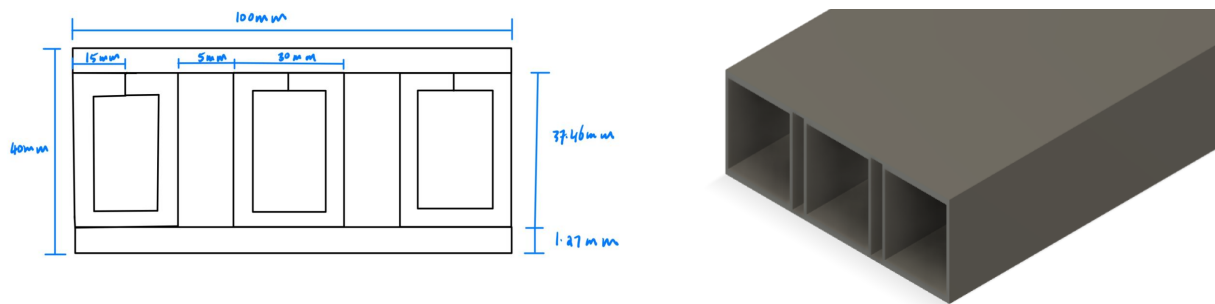
- $I = 0.418 \times 10^6 \text{ mm}^4$, $\bar{y} = 41.4 \text{ mm}$
- FOS against matboard tension failure = 16.69
- FOS against matboard compression failure = 3.53
- FOS against matboard shear failure = 5.52
- FOS against contact cement shear failure = 401
- FOS against matboard flexural buckling failure = 8.13
- FOS against matboard tip buckling failure = N/A because there are no tips on the top of the matboard, and tips at the bottom are in tension, thus buckling failure is not possible
- FOS against matboard web flexural buckling failure = 3.23
- FOS against matboard web shear buckling failure = N/A because no diaphragms are incorporated into the design
- Failure load = 1292 N
- Failure load, with a FOS of 2 considered due to possible construction errors: 646 N

Reason For Rejection:

- This design was created before the consideration of diaphragms for increasing the stiffness of the cross section. The nature of the cross-section design necessitates three separate pieces (the left, right, and in between the webs) to construct a diaphragm at one location. The folding of many diaphragm pieces contributes to useless material usage.
- This design was created before the consideration of matboard cutting. Although the design is feasible, many splice locations would arise, weakening the overall structure.

Design 2: Cross-section with multiple U-shaped webs

Visualization



Key parameter(s) altered

Three U-shaped webs were incorporated into the cross section instead of one, resulting in an inevitable tradeoff by decreasing height.

Justification

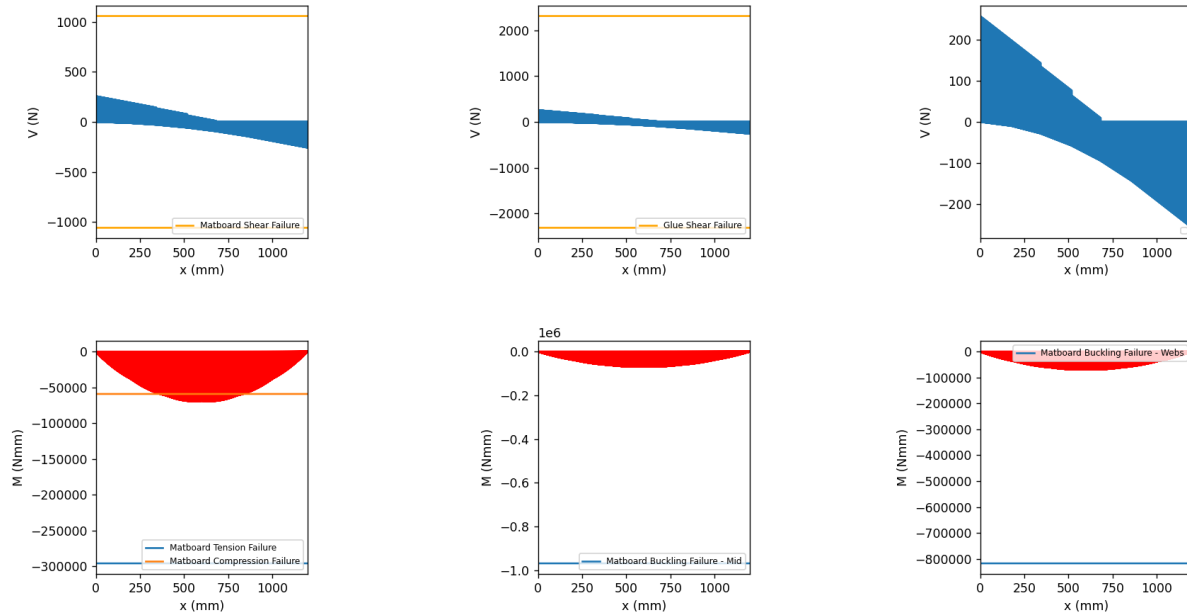
- Conceptually, having multiple vertical webs helps the cross-section to become sturdier, and resist bending moments better. However, there exists a trade-off between having more vertical segments and the decreasing height of the bridge because of the constraint placed on

matboard area. The distances between the centroidal axis of the overall cross-section and cross-section of individual rectangular areas also decrease, which decreases the second

$$\text{moment of area } I \text{ calculated through the parallel axis theorem } I = \sum_i^n \frac{b_i h_i^3}{12} + \sum_i^n b_i h_i (\bar{y}_i - \bar{y}).$$

This design concept serves to test the legitimacy of such a trade-off. Additionally, having three box girders as the cross section practically eliminates any possibility of incorporating diaphragms throughout the bridge, which is disadvantageous against high shear force.

SFDs and BMDs



Results

As shown from the values of factors of safety below, this bridge design will experience matboard compression failure with a train load of 400 N. This design concept demonstrates how increasing heights makes the bridge more resistant to such failures, in comparison to intuitively increasing the “sturdiness” by having multiple U-shaped vertical webs.

- $I = 3.18 \times 10^6 \text{ mm}^4$, $\bar{y} = 82.2 \text{ mm}$
- FOS against matboard tension failure = 4.26
- FOS against matboard compression failure = 0.852
- FOS against matboard shear failure = 4.11
- FOS against contact cement shear failure = 9.01
- FOS against matboard flexural buckling failure = 13.95
- FOS against matboard tip buckling failure = N/A because there are no tips on the flanges, therefore no buckling failure possible
- FOS against matboard web flexural buckling failure = 11.77
- FOS against matboard web shear buckling failure = N/A because no diaphragms are incorporated into the design

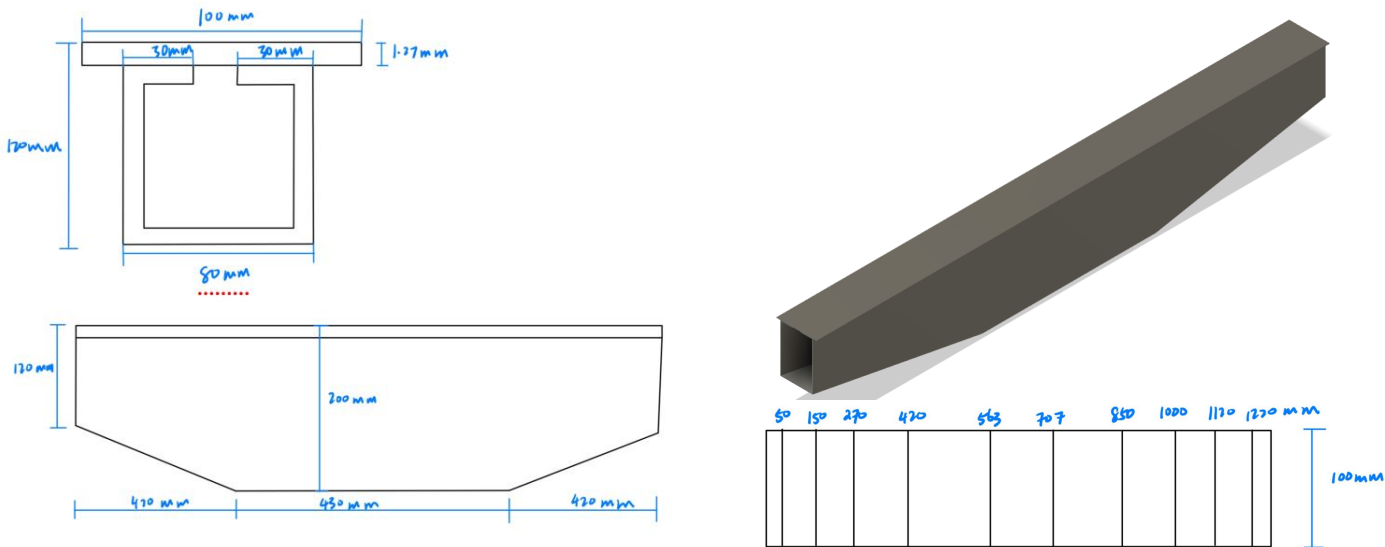
- Failure load = 341 N
- Failure load, with a FOS of 2 considered due to possible construction errors: 170.5 N

Reason For Rejection

- This design fails due to matboard compression, suggesting the importance of increasing web height h_{web} to increase the second moment of area of a cross-sectional area.

Design 3: Variable Bridge Height

Visualization



Key parameter(s) altered

- Return to box girder shape
- Increase width of glue tabs from 6.27 mm (design 0) to 30 mm
- Increase height from 120 mm to 200 mm in the middle section of the bridge (between 420 mm and 850 mm from the left support). The transition from 120 mm to 200 mm is a gradual, slope increase instead of step-size increase.
- Diaphragms incorporated throughout the bridge, denser diaphragms closer to the supports. The diaphragm locations from (distance from left support in mm): 50, 150, 270, 420, 563, 707, 850, 1000, 1120, 1220.

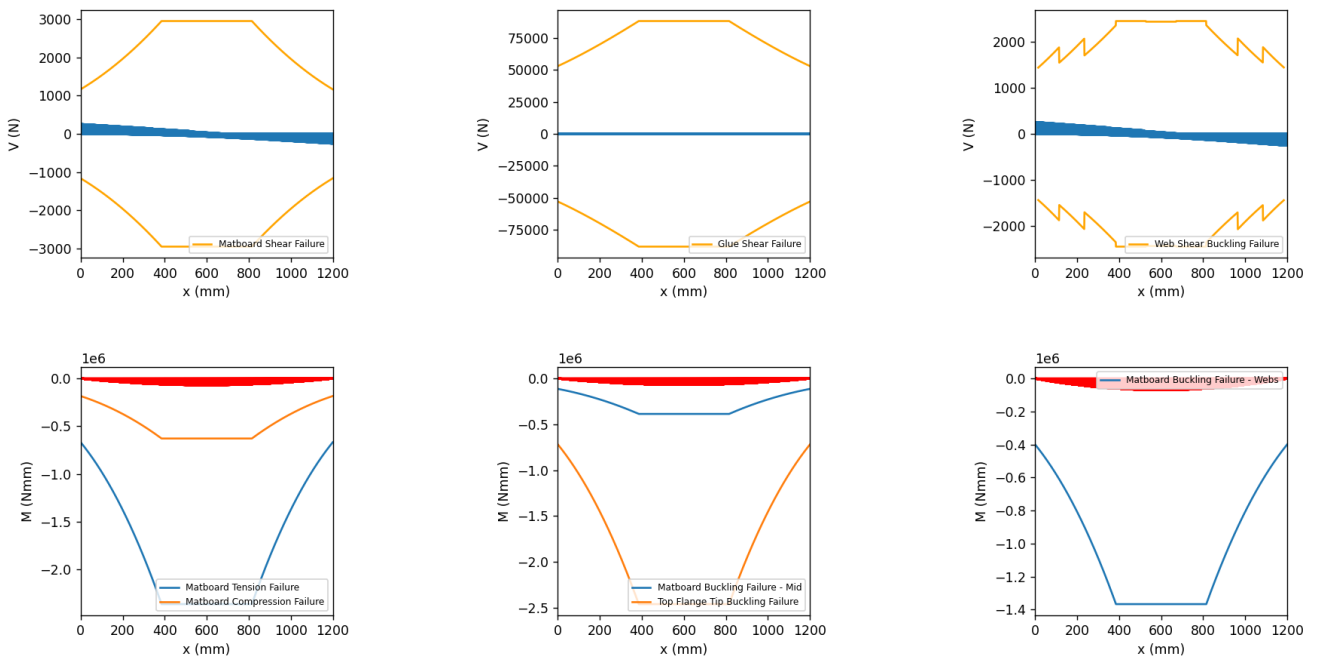
Justification:

- By graphing out V_{max} and M_{max} experienced by the bridge when the train passes through (symmetrical loading case of train), it is evident that the shear force is the highest near the supports (around 257 N) and moment peaks at around midspan (around 69445 Nmm). Ideally, the bridge shape in elevation view should resemble the graphs of V_{max} and M_{max} , but this is unfeasible because V and M peak at distinct locations. As a result, the bridge in the middle section is given a higher height of 200 mm to resist bending moments, and a relatively denser diaphragm distribution is designed around the supports to resist shear

forces. Since shear failure equations learned in this course did not take diaphragms into consideration, the actual shear failure load is estimated to be higher than the computed failure load.

- Several trade-offs were realized when altering parameters for this cross-section design and the best parameters were chosen for this design:
 - When increasing the height of the cross-section, the second moment of area (I) increases roughly proportional to h^3 , as per the formula for I for rectangular cross sections $I = \frac{bh^3}{12}$, making the bridge more resistant to both shear and moment. The value of the first moment of area (Q) increases roughly proportional to h^2 , and location of the centroidal axis and glue heights also shifts. Whereas, flexural stress calculated through $\sigma = \frac{My}{I}$ seems to always decrease in response to increasing heights, shear stress calculation $\tau = \frac{VQ}{Ib}$ shows an ambiguous trend because of the opposing Q increase and I increase effects. This is a reminder that sometimes higher heights do not always return the maximum failure force, and an iterative optimization process through which a variety of heights (i.e. 80mm, 100 mm, ..., 160 mm, 180 mm) is needed.
 - When increasing the height of the cross-section, the second moment of area (I) increases, making the bridge design more resistant to both shear and moment. However, the webs become more susceptible to web flexural and shear buckling because the $\frac{t}{h_{\text{web}}}$ term in buckling failure equations becomes smaller with greater h_{web} , and consequently, the FOS due to those failures decreases.
 - To increase the FOS for tip buckling on the top flange (i.e. increase $\frac{t_{\text{flange}}}{b_{\text{out}}}$), the design could have the web bending outward instead of inward to decrease tip width. However, this comes at the expense of increasing the spacing between two glue tabs, which ends up decreasing the FOS for flange buckling (decreased $\frac{t_{\text{flange}}}{b_{\text{in}}}$) in practice, even though the glue tab widths are not factored in FOS calculations. To improve FOS against flange buckling, the width of the flange should be designed to be smaller, which in turn increases the tip width and makes the bridge more vulnerable to tip buckling.
 - Material-wise, having higher heights decreases the number of diaphragms that could be incorporated into the design, sacrificing strength against shear force at the supports for strength against moment in the middle of the bridge.
- After maneuvering with multiple heights, tip widths, and flange widths, design 3 has the greatest failure load amongst its family of similar designs. The heights explored include 120 mm at supports and 200 mm at midspan, 120 mm at support and 160 mm at midspan, 140 mm at support and 160 mm at midspan, 140 mm at support and 180 mm at midspan. The glue tab widths explored are in the range of 5 mm to 30 mm in increments of 5 mm. The top flange widths explored are in the range of 70 mm to 90 mm in increments of 5 mm.

SFDs and BMDs:



Results:

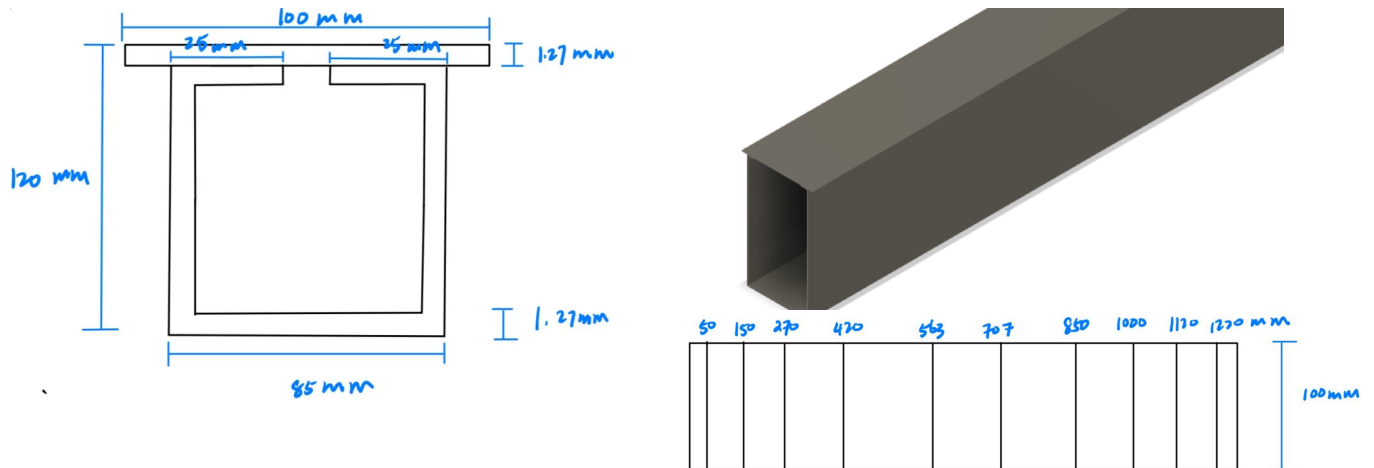
- At support, $I = 1.340 \times 10^6 \text{ mm}^4$, $\bar{y} = 69.9 \text{ mm}$;
At max height, $I = 5.28 \times 10^6 \text{ mm}^4$, $\bar{y} = 87.2 \text{ mm}$
- FOS against matboard tension failure = 34.1
- FOS against matboard compression failure = 9.05
- FOS against matboard shear failure = 4.53
- FOS against contact cement shear failure = 206
- FOS against matboard flexural buckling failure = 5.56
- FOS against matboard tip buckling failure = 35.4
- FOS against matboard web flexural buckling failure = 19.67
- FOS against matboard web shear buckling failure = 5.69
- Failure load = 1812 N
- Failure load, with a FOS of 2 considered due to possible construction errors: 906 N

Reason For Rejection

- This design was created before the consideration of matboard cutting. Although the design returns a much higher failure load in comparison to other designs, it is not feasible height-wise.
- The diaphragm construction of this bridge design is also challenging, with lots of room for irreversible errors. Not only is there very little leftover matboard for splice reinforcements, the variable height at the left and right of diaphragms necessitates diaphragms with variable heights throughout the bridge as well. It was decided that it would not be an optimal use of a matboard.

Design 4: Box Girder With Constant Height

Visualization



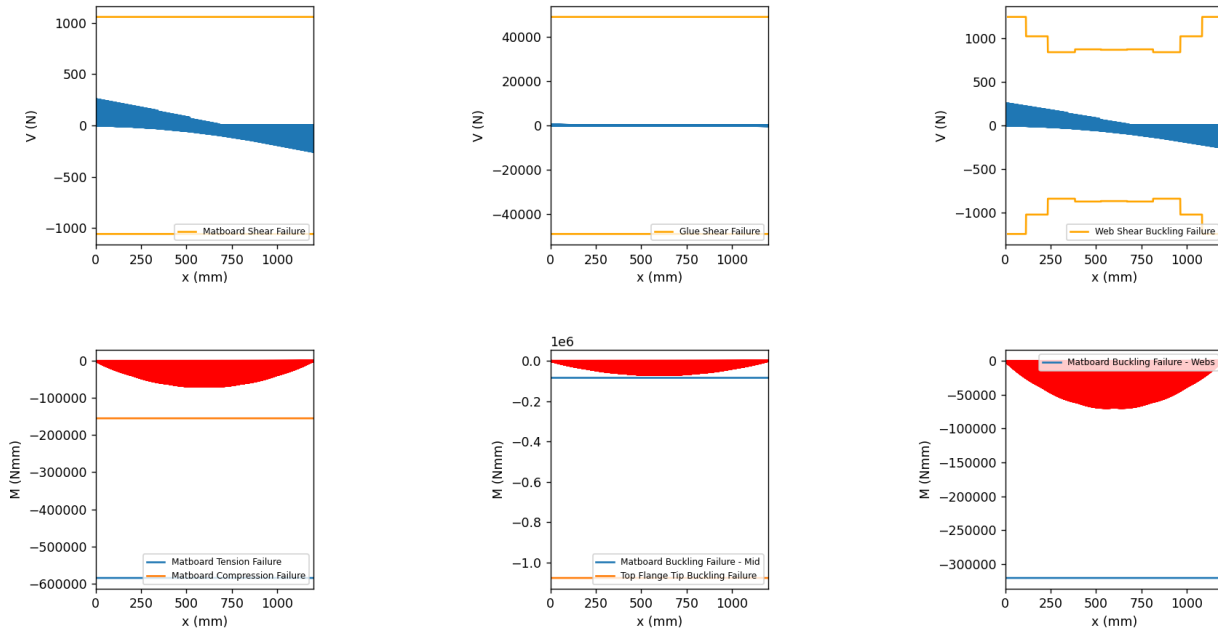
Key parameter(s) altered:

- Increase in width of bottom flange from 80 mm to 85 mm (in comparison to design 3)
- Decrease in width of glue tabs from 30 mm to 25 mm (in comparison to design 3)

Justification

- Despite the more complex design involving variable height in design 3, it is not feasible from a constructive point of view. Also, the minimum factor of safety is always obtained close to the two supports instead of at midspan because the ratio between failure stresses and actual stress is the lowest at supports. Therefore, according to $FOS = \min\{FOS(\text{tension}), FOS(\text{compression}), \dots\}$, FOS at supports (where there is no variable height) always dominates the FOS of the entire bridge. Thus, a variable height is not completely necessary if the bridge has a dominating failure mode that does not vary because of greater heights in the middle. Design 4 is proposed with the intention of simpler bridge construction yet higher possible shear resistance at the supports.
- Cross-section wise, the only parameters changed from design 3 to design 4 is a higher web width (85 mm) and lower folded length of the web at the top flange (25 mm). Even though a lack of length variation causes the FOS against moment failures to decrease, an improved FOS for matboard shear failure shall hopefully still dominate the overall FOS of this design. As shown from designs 3, matboard shear failure is most likely the dominant form of bridge failure for a box girder cross-section shape.

SFDs and BMDs:



Results:

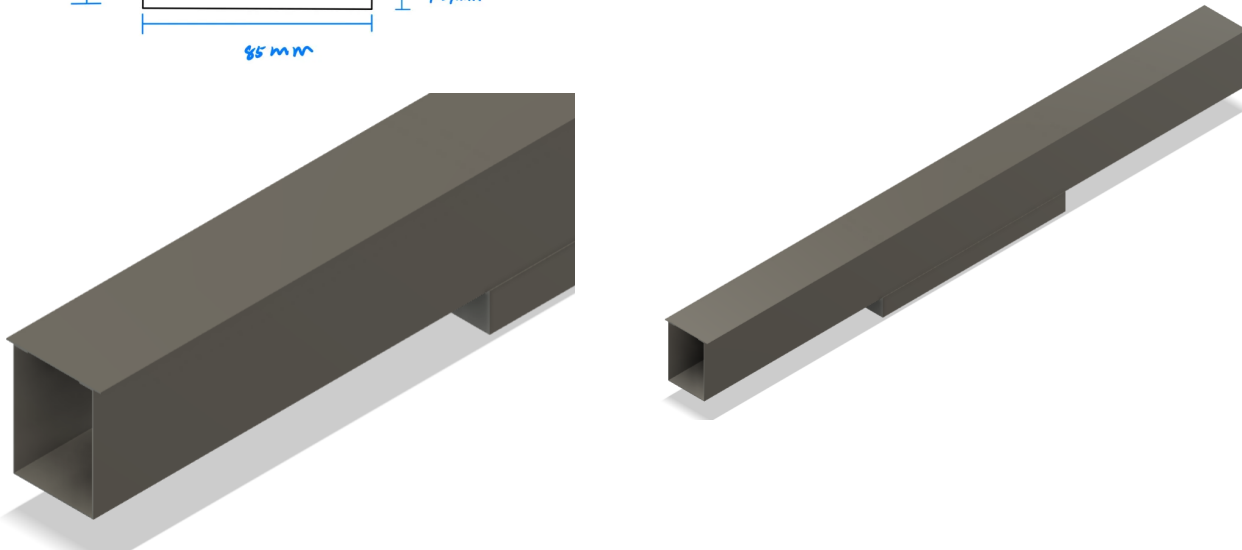
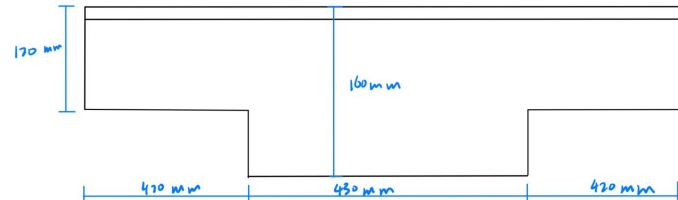
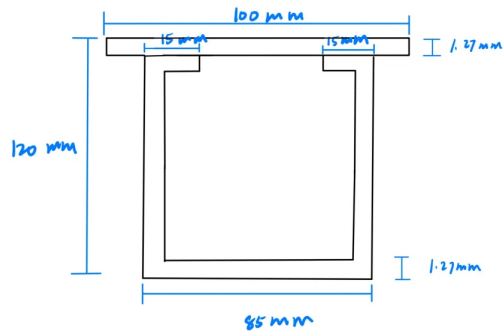
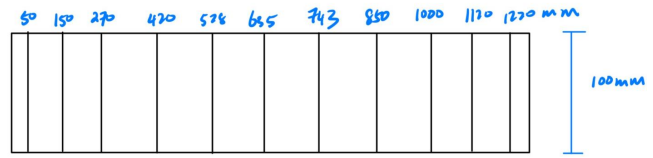
- $I = 1.333 \times 10^6 \text{ mm}^4$, $\bar{y} = 68.3 \text{ mm}$
- FOS against matboard tension failure = 8.43
- FOS against matboard compression failure = 2.23
- FOS against matboard shear failure = 4.11
- FOS against contact cement shear failure = 190.1
- FOS against matboard flexural buckling failure = 1.208
- FOS against matboard tip buckling failure = 15.51
- FOS against matboard web flexural buckling failure = 4.61
- FOS against matboard web shear buckling failure = 4.69
- Failure load = 483 N
- Failure load, with a FOS of 2 considered due to possible construction errors: 242 N

Reason For Rejection

- Contrary to predictions, even though the factor of safety against shear failure dominates design 3, factor of safety against moment failure dominates design 4 in top flange buckling, which decreases the failure load the bridge can resist.

Design 5: Box Girder With Variable Heights

Visualization



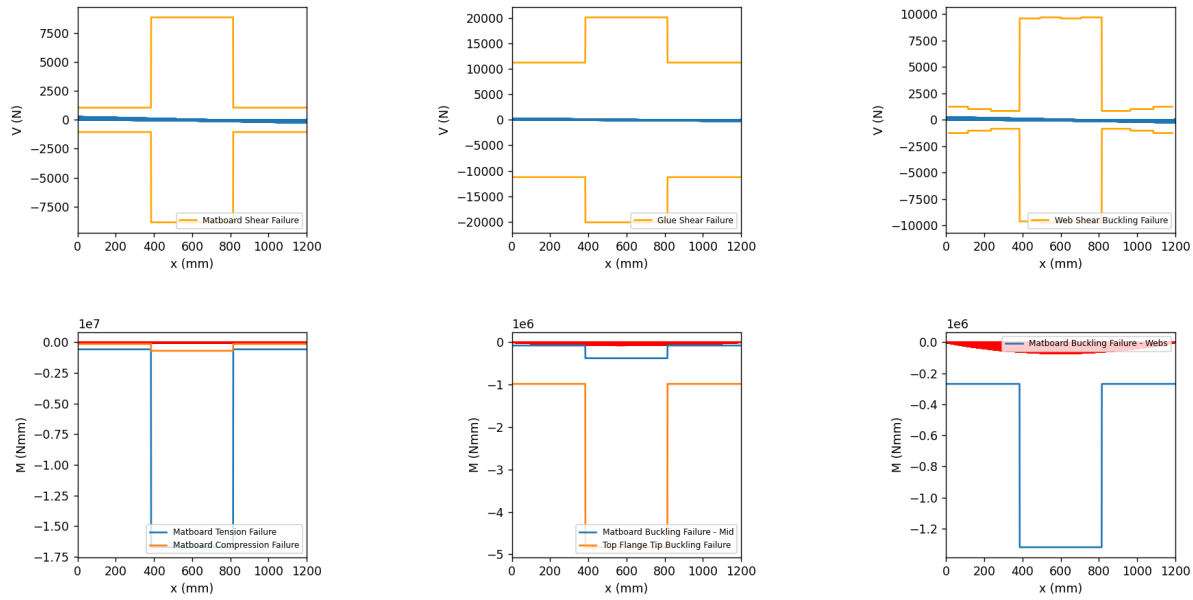
Key parameter(s) altered

- Decrease in width of glue tabs from 20 mm to 15 mm (in comparison to design 4)
- Incorporate step-like variation in height throughout the bridge

Justification

- The failure of design 4 due to bending moments suggests a variable height for design 5. However, because of the difficulty of construction of design 3, design 5 is adapted to have stepwise increase in height.

SFDs and BMDs



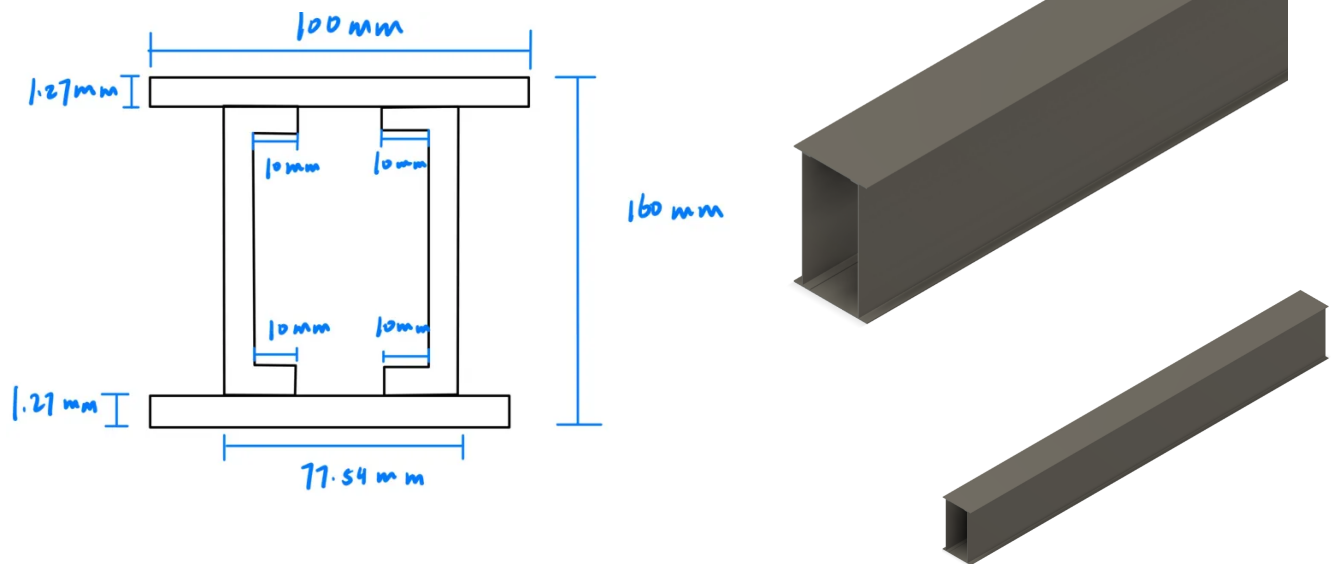
Results

- At supports, $I = 1.267 \times 10^6 \text{ mm}^4$, $\bar{y} = 66.1 \text{ mm}$
At max heights, $I = 6.24 \times 10^6 \text{ mm}^4$, $\bar{y} = 74.4 \text{ mm}$
- FOS against matboard tension failure = 9.50
- FOS against matboard compression failure = 2.33
- FOS against matboard shear failure = 4.10
- FOS against contact cement shear failure = 43.7
- FOS against matboard flexural buckling failure = 1.260
- FOS against matboard tip buckling failure = 16.22
- FOS against matboard web flexural buckling failure = 4.43
- FOS against matboard web shear buckling failure = 4.68
- Failure load = 505 N
- Failure load, with a FOS of 2 considered due to possible construction errors: 253N

Reasons For Rejection

- Even though the design 5 significantly improves the factor of safety against bending moment failure at midspan, this design still fails due to bending moment at supports. Since designs 4 and 5 have the same cross-section at supports, their factors of safety against shear are the same.

Design 6: C-Shaped Webs Shapes



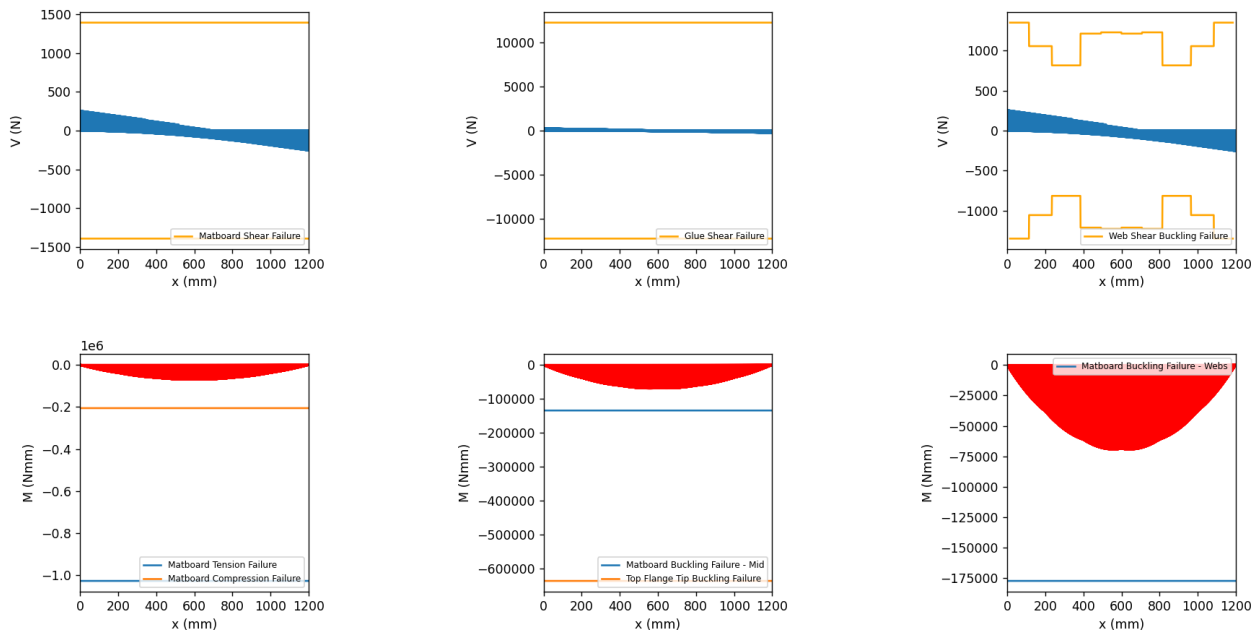
Key parameter(s) altered

- Change cross section from U-shaped box girder to two C-shaped webs
- Decrease width of the glue tab from 15 mm to 11.27 mm (in comparison to design 5)
- Decrease width of two webs from 85 mm to 77.54 mm (in comparison to design 5)

Justification

- Design 6 takes the construction process, or more specifically, the cutting of the matboard piece into consideration. Even though previous designs may have leftover areas, the areas may be shaped into a long slim rectangle to be put to use for any purposes such as diaphragms, splice reinforcements, etc. As a result, design 6 has a constraint of 180 mm on the entire length of C shape (including the vertical bridge and folded length), because otherwise there will be many other splices in the bridge in addition to the ones that are due to the inability of the short matboard length to span a 1200 mm gap.
- Design 6 changes the width of the web (bottom flange) to 77.54 mm to adapt to the width of the train so that the points of contact the train wheels make with the top flange are directly supported by the vertical pieces of the web underneath.
- One significant reason that C-shaped webs are superior over the box girder cross-section is that the left and right webs of a C-shaped cross section can incorporate splices at various locations as they are cut out separately, thus propagating the weakness of the bridge to not a singular point but multiple locations. On the other hand, for a box girder which is folded to form the left and right webs, there is only one splice location throughout the bridge span, making that specific location the most susceptible and weaker than any location on the C-shaped bridge that has multiple splice locations.

SFDs and BMDs



Results:

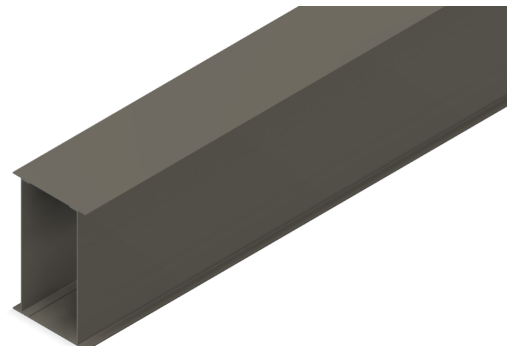
- $I = 2.74 \times 10^6 \text{ mm}^4$, $\bar{y} = 80.0 \text{ mm}$
- FOS against matboard tension failure = 14.77
- FOS against matboard compression failure = 2.95
- FOS against matboard shear failure = 5.43
- FOS against contact cement shear failure = 47.6
- FOS against matboard flexural buckling failure = 1.936
- FOS against matboard tip buckling failure = 9.17
- FOS against matboard web flexural buckling failure = 2.55
- FOS against matboard web shear buckling failure = 4.57
- Failure load = 774 N
- Failure load, with a FOS of 2 considered due to possible construction errors: 384 N

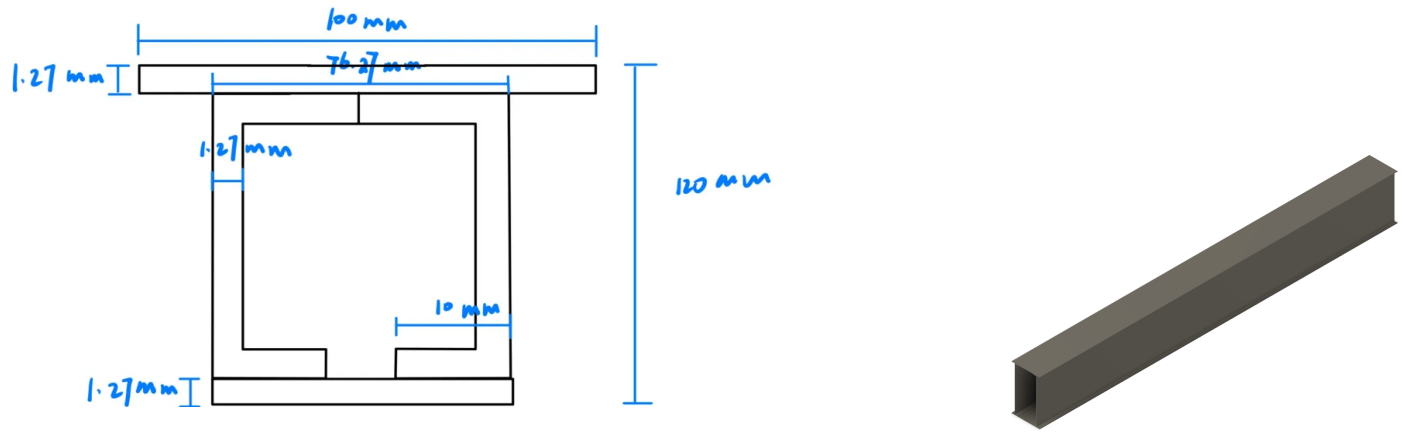
Reasons For Rejection

- All prior designs, including design 6, have consistently had flexural buckling failure as the reason for their failure. Realizing this limitation, design 7 improves from design 6.

Design 7: Double Flange Width

Visualization





Key parameter(s) altered

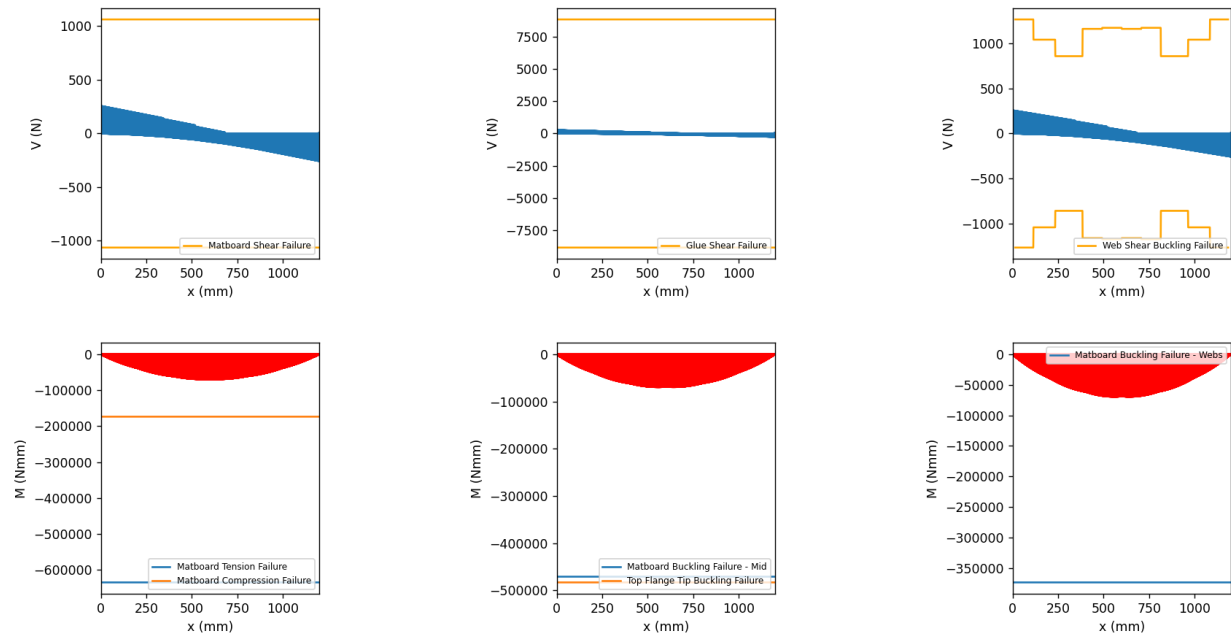
- Increase width of the glue tab from 11.27 mm to 38.1 mm (in comparison to design 6) so that two glue tab widths combined effectively doubles the thickness of top flange
- Decrease width of the bottom flange to be the same as distance between webs

Justification

- Past designs all indicated failure because of buckling of top flange, whose failure mode is governed by the equation $\sigma = \frac{4\pi^2 E}{12(1-\mu^2)} \left(\frac{t}{b_{flange}}\right)^2$. There are two ways to increasing σ : either decrease b_{flange} or increase t . One of the constraints applied to all designs is that the flange should at least be as wide as train width, otherwise tip buckling becomes dangerously likely. Therefore, the only approach to increasing σ is to add another layer to the top flange such that the thickness is doubled. With C-shaped webs, the glue tab widths were increased such that they close any gap in between, effectively forming the second layer for top flange. The glue tab width at the bottom was reduced from 11.27 mm to 10 mm to fit the constraint on the maximum length each C-shape could have (~180 mm). Other parameters for the cross-sectional remain identical to design 6.

After converging, our two major designs considered were design 7 and design 8, as mentioned below.

SFDs and BMDs



Results

- $I = 1.468 \times 10^6 \text{ mm}^4$, $\bar{y} = 69.3 \text{ mm}$
- FOS against matboard tension failure = 9.15
- FOS against matboard compression failure = 2.50
- FOS against matboard shear failure = 4.14
- FOS against contact cement shear failure = 34.3
- FOS against matboard flexural buckling failure = 6.78
- FOS against matboard tip buckling failure = 6.96
- FOS against matboard web flexural buckling failure = 5.38
- FOS against matboard web shear buckling failure = 4.77
- Failure load = 1001 N
- Failure load, with a FOS of 2 considered due to possible construction errors: 501 N

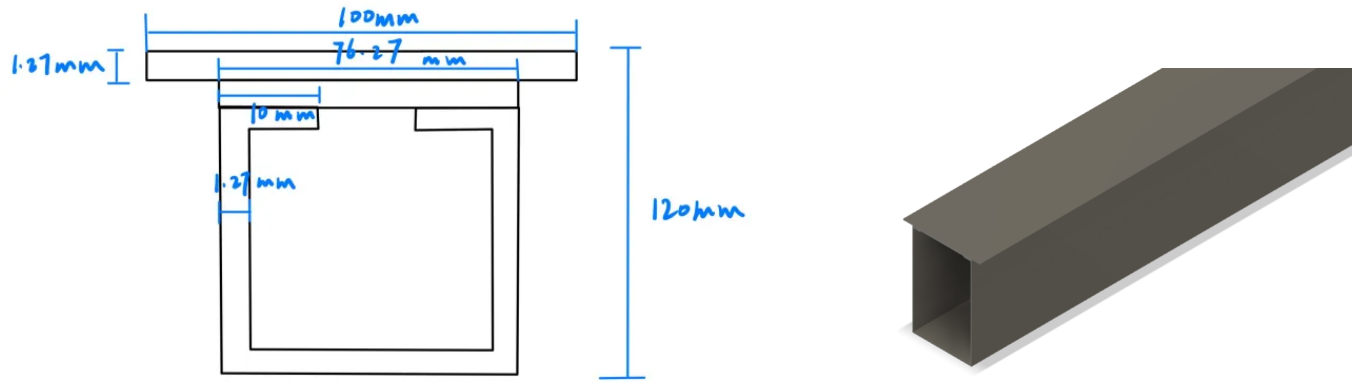
Reasons For Rejection

- Design 8 has a higher failure load in comparison to design 7.

Design 8 (Final Design):

Visualization





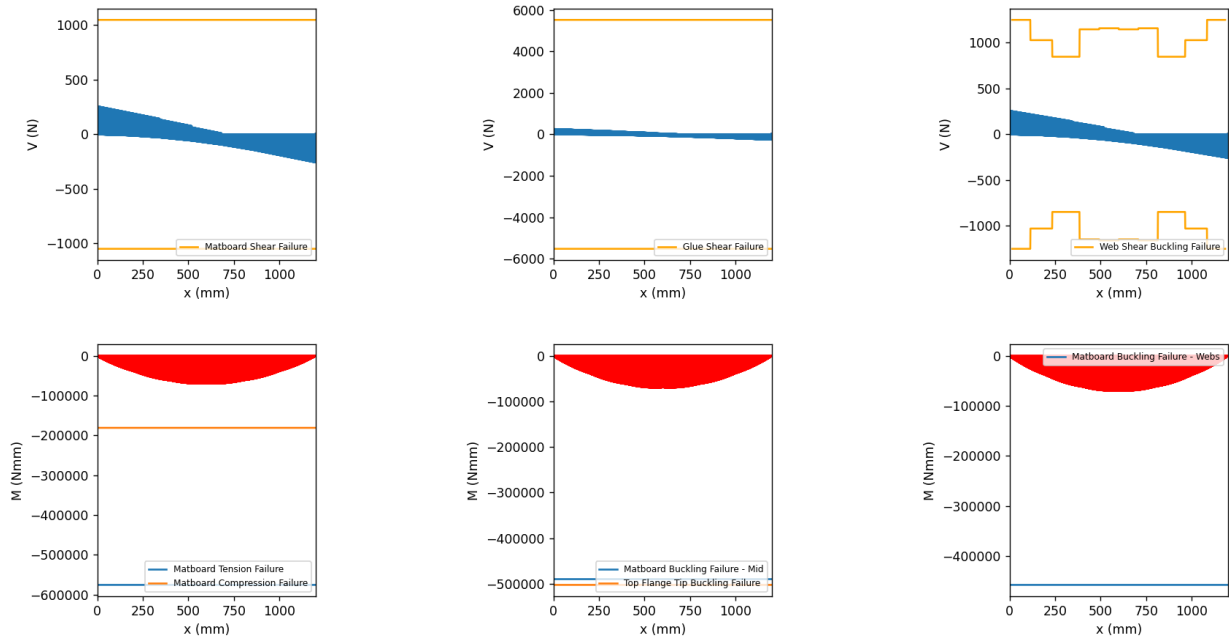
Key parameter(s) altered

- Use two layers of matboard as top flange instead of C-shaped webs covering up the gap length between the glue tabs
- No bottom flange is needed, as opposed to design 7 with C-shaped webs

Justification

- From design 7, it is realized that the matboard bridge fails due to flexural compression at the top of the flange, after the issue of top flange buckling has been improved. The calculation for the actual compressive flexural stress in the top flange is $\sigma = \frac{My_{top}}{I}$, and decreasing y_{top} (which represents distance from top flange to centroidal axis \bar{y}) helps decrease the actual stress, thus increasing FOS for flexural compression. Design 8 could almost be viewed as identical to design 7 except that the bottom flange in design 7 is moved to above the glue tabs in the top flange in design 8, and the bottom end of the C-brackets are connected. As a result of increased area on top, the centroidal axis of the cross-section shifts up, decreasing y_{top} and σ and thus improving the FOS for flexural compression.

SFDs and BMDs



Results

- $I = 1.407 \times 10^6 \text{ mm}^4$, $\bar{y} = 73.3 \text{ mm}$
- FOS against matboard tension failure = 8.29
- FOS against matboard compression failure = 2.60
- FOS against matboard shear failure = 4.08
- FOS against contact cement shear failure = 21.5
- FOS against matboard flexural buckling failure = 7.06
- FOS against matboard tip buckling failure = 7.24
- FOS against matboard web flexural buckling failure = 6.60
- FOS against matboard web shear buckling failure = 4.70
- Failure load = 1041 N
- Failure load, with a FOS of 2 considered due to possible construction errors: 521 N

3 Construction Process

Maintenance of Construction Environment

The bridge construction took place at two different locations on November 25th: Galbraith building room 227 (4 p.m. to 9 p.m.) and the Sandford Fleming engineering pit afterwards. Throughout bridge construction, trash bags were set up to immediately dispose of trash and waste materials to maintain a clean and safe work environment (Fig. 1). The pictures below

showcases the precaution taken by the team during construction and the state of the work environment cleanup.



bridge
after

Figure 1: Trash bags were prepared and used to dispose of waste throughout construction. (Nov. 25th 4:22 p.m)

Figure 2: State of work table in Galbraith Room 227 after work session and cleanup. (Nov. 25th 8:33 p.m). All the garbage and scraps were collected in the white bag, as shown above.



Figure 3: Plastic bags were set up underneath the bridge during its gluing process. (Nov. 25th 8:43 p.m)

Figure 4: State of work table in Sandford Fleming pit post work session and cleanup. (Nov. 26th 1:07 a.m)

Matboard Layout

Since the matboard area constraint is significant to bridge cutting and design, the digital tool *Cutlist Optimizer* was used to optimize and generate the layout of matboard cutting for the finalized bridge design (Fig. 5) (also shown on Engineering Drawings). The proposed design includes all necessary components of the bridge (flanges, box girder webs, and anticipated 11 flanges), and the leftover areas were used to patch up the splices throughout the bridge.

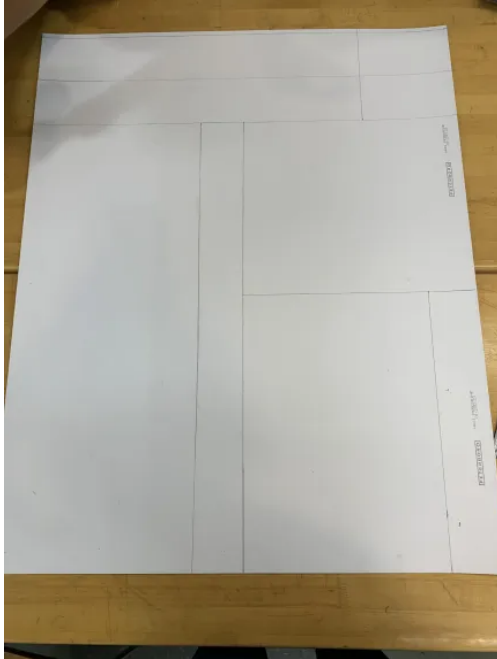
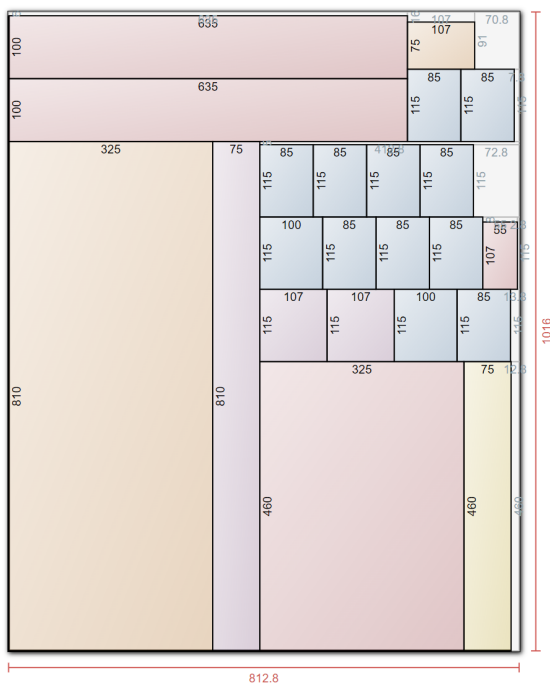


Figure 5: ‘Cutlist Optimizer’ layout for matboard cutting

Figure 6: Cut lines drawn out in accordance with results taken from Cutlist Optimizer (taken on November 26th 5:35 p.m.)

Matboard Measurement and Cutting

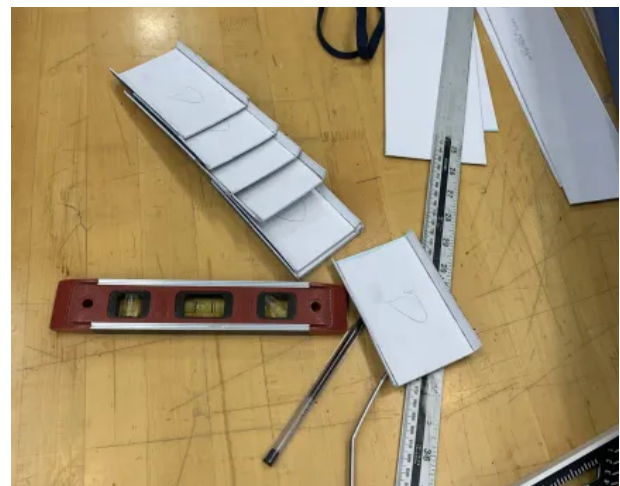
All matboard measurements were made using a meterstick and a tape measure. To ensure that various lines were perpendicular, a leveler was held against the matboard edge, and an L ruler was held against the leveler to ensure right angles in cut lines. All cutting was performed by a xacto knife upon two pieces of sacrificial wood.

Given the nature of our final design, folding the matboard was required and thus necessitates scoring prior to folding. Various tools were attempted for effectiveness of scoring, including ball pen tips, pencils, cards, and keys. Ultimately, house keys were chosen to score the matboard and create the groove, and the scored matboard was folded up against the straight edge of a level. Our box girder shape required four folds (twice at corners of bottom flange and twice at glue

tabs); diaphragms required two folds to become attached to the vertical wall. All folds have scoring performed prior.



Figure 7: Matboard cutting process (Nov. 25th 7:23 p.m)



Figures 8 and 9: Scoring and folding of box girder shape and diaphragms (Nov 25th 8:25 p.m)

Gluing Process

Throughout the gluing process, papers were folded as applicators to spread glue over matboard surfaces. We first glued together the two U-shaped webs and reinforced the splice location with extra matboard on the interior (Fig. 10). The folded diaphragms were then glued to one side of the web to avoid mistakes when glued to both sides of the web at once (Fig. 11). After one side

of the diaphragms was secured, the other side was matched and glued to correct locations on the opposite side of the U-shaped web shape (Fig. 12). Simultaneously, the lower top flange was patched at its splice, but during its gluing onto the base and diaphragms (i.e: the glue tabs), we ensured different locations of splice to not expose a singular weakest point in our bridge (Fig. 13). The final piece of gluing performed was to put the higher top flange onto the lower top flange to complete the bridge design. Weights were applied upon the bridge to ensure uniform pressure for contact cement to take effect (Fig. 13). The bridge piece is completed approximately 110 hours prior to testing.



Figure 10: A picture showing location of splice in the U-shaped webs (Nov. 25th 8:43 p.m).



Figure 11: Individual diaphragms laying on table based on the order in which glue was applied (Nov. 25th 10:23 p.m).



Figure 12: Diaphragm gluing process (Nov. 25th 10:51 p.m) Note, only the diaphragms were glued away from the garbage bag covering as the bag got into the way of maneuvering the bridge appropriately.

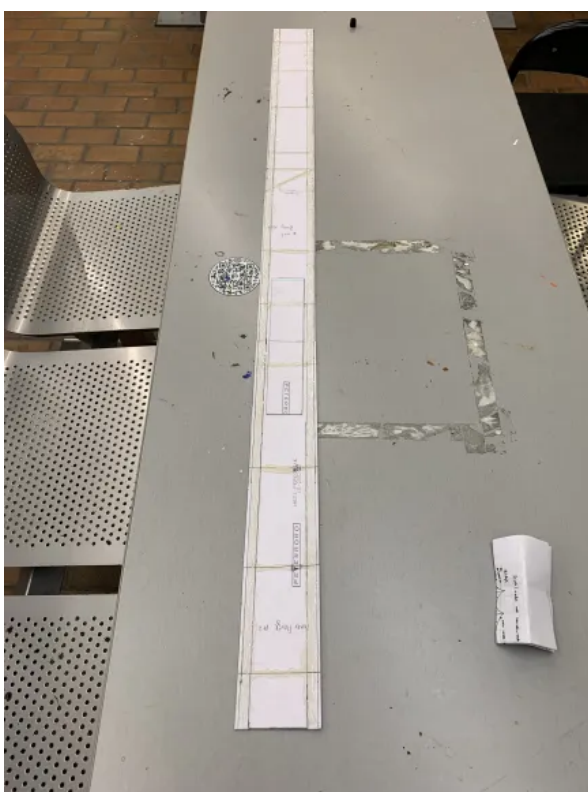


Figure 12: Diaphragm gluing process (Nov. 25th 10:51 p.m). Due to an issue with space on one table, the inner flange was set to dry. The surface was carefully wiped down afterwards.



Figure 13: Heavy wood sits on top of the completed bridge for uniform pressure (Nov. 26th 12:14 p.m)

*Note, all surfaces were wiped down after construction using alcohol-based cleaning wipes and wet and dry paper towels.